SUPPLEMENTARY MATERIAL

FOR

THE LIPID-BINDING DOMAIN OF WILD TYPE AND MUTANT ALPHA-SYNUCLEIN: COMPACTNESS AND INTERCONVERSION BETWEEN THE BROKEN- AND EXTENDED-HELIX FORMS.

Elka R. Georgieva[1], Trudy F. Ramlall[2], Peter P. Borbat[1], Jack H. Freed[1], David Eliezer[2].

From [1]Department of Chemistry and Chemical Biology, Cornell University, Ithaca, NY 14853; [2]Department of Biochemistry and Program in Structural Biology, Weill Cornell Medical College, 1300 York Avenue, New York, NY 10065

Running Title: Helix interconversion of alpha-synuclein

Address correspondence to: dae2005@med.cornell.edu; jhf3@cornell.edu

I. DEER results from titration experiment on spin-labeled at positions 24 and 61 WT αS

A series of samples made from WT αS reconstituted into 40 mM SDS solutions were prepared by gradually decreasing the protein concentration in the range of 100 to 20 μM, yielding protein-to-SDS molar ratios in the range of 1:400 to 1:2000. The time-domain pulsed dipolar signals from these samples and the reconstructed distances are plotted in Fig. S1 left and right panels, respectively (solid lines). Distances and distance distributions were analyzed according to standard protocol: first, we applied the Tikhonov L-curve method (Ref. S1), and the $P(r)$'s obtained were then used as seeds for the MEM refinement that include base-line correction (Ref. S2). Further, we applied the two-Gaussian model to estimate the populations of the short- and long-distance conformers. The envelopes of the theoretical two-Gaussians, which are the best fits to the experimentally reconstructed distributions, are shown in Figure S1 (dashed lines). The parameters, which were used in two-Gaussians approximation, are summarized in Table S1.

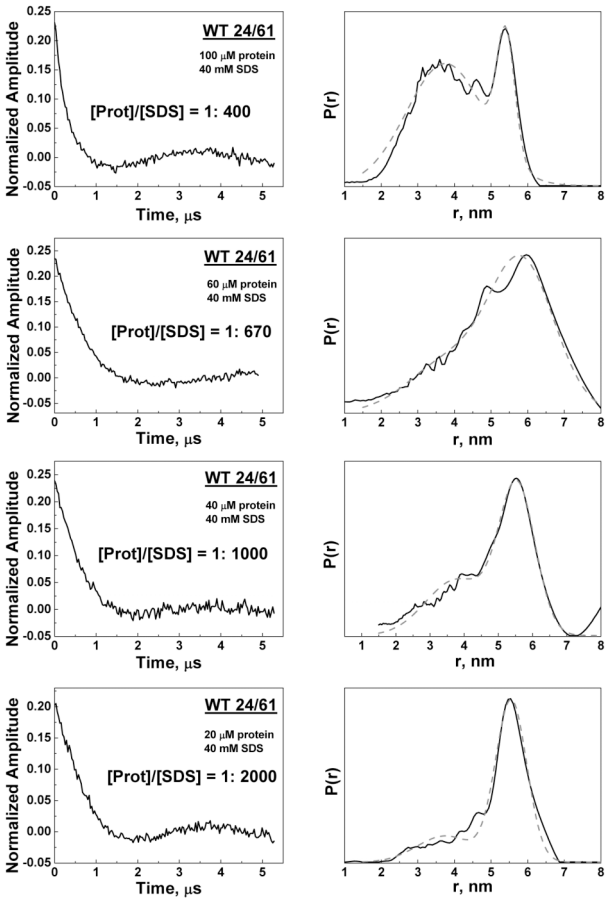

Figure S1. Experimental time-domain data (left panel) and reconstructed distances and distance distributions (right) from spin-labeled at positions 24 and 61 WT αS, which was reconstructed into SDS solutions with SDs final concentration of 40 mM. Protein concentration was varied in the range of 100 to 20 μM, yielding protein-to-SDS molar ratios in the range of 1:400 to 1:2000. Envelopes of two-Gaussians distributions, which were used to approximate the experimentally obtained distance distributions, are plotted in gray dashed lines (right panel).

Table S1. Two-Gaussian model fitting parameters (average distance R and ΔR (FWHM) in nm) used to approximate distance distributions for WT αS, spin-labeled at positions 24 and 61. The protein was reconstituted at concentrations in the range of 20 to 100 μM into SDS solutions with SDS concentrations of 40 mM. The protein-to-SDS molar ratios are given in the table.

[Protein]	[Protein] to [SDS] ratio	R	ΔR	Long Dist., %
100 μM	1:400	3.75 5.4	2.5 0.6	19
60 μM	1:670	3.85 5.8	2.6 2.1	30
40 μM	1:1000	3.8 5.55	2.2 1.25	61
20 μM	1:2000	3.75 5.55	1.8 1.0	77

II. DEER measurement on magnetically diluted samples

We performed experiments on magnetically diluted samples to verify that the short-to-long distance transition observed with the increase in the detergent-to-protein molar ratio is not due to protein aggregation, but represents intrinsic properties of αS variants to interconvert between two structural conformations: broken and extended helix. For this purpose we performed magnetic dilutions by adding to the samples of spin-labeled A30P mutant diamagnetic cysteine-less A30P protein. A30P was chosen because of the good signal-to-noise ratio for the diluted sample. Each diluted sample was prepared from 15 μM of spin-labeled protein stock, labeled at positions 24 and 72, and 25 μM solution of unlabeled protein. This corresponds to a 40 μM concentration of total protein, which was then compared with undiluted sample prepared from 40 μM spin-labeled protein stock solution. The samples were then reconstituted into SDS solutions using two different concentrations of SDS. In the case of protein aggregation, wherein its effects show up in undiluted samples, but less so in diluted, their difference should be clearly visible in the time-domain signals (and reconstructed distance distributions).

<u>Magnetically diluted A30P mutant tested in 5 mM and 40 mM SDS.</u>

For this mutant the magnetically diluted samples we obtained yielded time-domain DEER signals with good signal-to-noise ratio sufficient for a detailed analysis. The time-domain data were normalized to unity at zero time and the baselines were subtracted out, leaving just the intramolecular contributions to the signal. The amplitude of the remaining signal after the subtraction ("dipolar signal amplitude" or "modulation depth") depends strongly (Ref. S3) on the number of spins in the aggregate. Since this number becomes considerably lower (by a factor of ~2.7) in the case of magnetic dilution used, the amplitudes in this case will become smaller by about the same factor. Fig. S2, clearly shows that this is not the case. On the contrary, there is considerable similarity between the data from magnetically diluted and non-diluted samples. Minor differences could

however be noticed in the case of protein in 40 mM SDS. These differences may be attributed to small uncertainties of instrumental origin, base-line subtraction residuals, and maybe a small extent of protein aggregation.

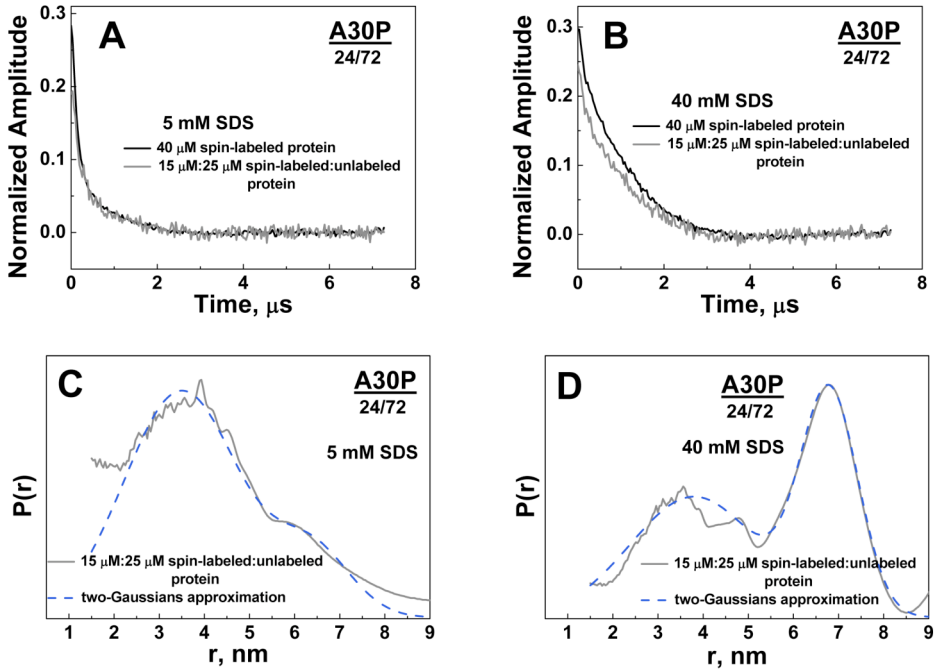

Figure S2. The results from the DEER measurements on magnetically diluted samples of A30P mutant for 40 μM total protein. The upper panels compare base-line subtracted time-domain DEER signals from the standard (black) and magnetically-diluted (gray) protein samples prepared in 5 mM (protein-to-SDS molar ratio of 1:125) (A) and 40 mM SDS (protein-to-SDS molar ratio of 1:1000). (B). The lower panels show the reconstructed distance distributions refined by MEM (gray lines) plotted together with two-Gaussian approximations (blue dashed lines) for the two cases of magnetically diluted protein in 5 mM SDS (C) and 40 mM SDS (D).

The protocol, which was described in the first section of the supplementary material and experimental procedures in the main text, was used to analyze the inter-spin distances and distance distributions. The MEM-refined distance distributions are shown in Fig. S2, lower panel (gray lines), for the cases of 5 mM (C) and 40 mM (D) SDS. The distance distributions unambiguously are bimodal and fully consistent with those found in magnetically non-diluted samples (cf. Fig. 4 in the main text). The two-Gaussian model was applied to estimate the

populations of the short- and long-distance conformers. The shapes of two-Gaussian distributions are plotted in blue dashed lines in Fig. S2, (C, D).

In order to estimate the ratio of the two components, we compared the parameters obtained in approximating the distance distribution with the two-Gaussian model (cf. below) for magnetically non-diluted samples to those used in the case of magnetically diluted samples. These parameters are compiled into Table S2.

Table S2. Two-Gaussians model fitting parameters [average distance, *R*, and width, Δ*R* (FWHM)] used to approximate distance distributions for magnetically non-diluted and diluted A30P mutant. Nitroxide spin-labels were introduced at positions 24 and 72. The protein was reconstituted with total concentration of 40 μM into SDS solutions at SDS concentrations of 5 and 40 mM. The Protein-to-SDS molar ratios are also shown.

[SDS]	[Protein] to [SDS] ratio	Magnetically non-diluted Protein			Magnetically diluted protein		
		R	Δ*R*	Long Dist., %	*R*	Δ*R*	Long Dist., %
5 mM	1:125	3.2	2.3	20.5	3.5	3.0	16
		6.3	2.7		6.3	2.0	
40 mM	1:1000	3.8	3.7	48	3.8	3.3	45
		6.8	1.3		6.8	1.5	

The fitting parameters used to analyze the distance distribution from magnetically diluted and non-diluted samples are very close. It should be noted that this is good evidence for the high reproducibility of our experimental data.

II. Calculations of the theoretical end-to-end distances in WT αS and mutants in free state in solution based on the model accounting for chain stiffness:

We used the equation for the Gaussian distribution of the root-mean-square end-to-end distance for a random walk model of polypeptide chain with stiffness,

which was previously applied to αS by Sung and Eliezer [S4]. A modification was introduced to account for the length of spin-labeled side-chains. The end-to-end distance is given by

$$\left\langle r^2 \right\rangle = nl^2 \left[\frac{1+\alpha}{1-\alpha} - \frac{2\alpha(1-\alpha^n)}{n(1-\alpha)^2} \right] + 2\left\langle L^2 \right\rangle \qquad \text{(S1)}$$

where r is the distance between the nitroxides moieties of the spin labels; n is the number of connecting chain links, equal in our case to the number of peptide segments that also include two cysteine side chains to which nitroxides are attached; l is the average length of the peptide bond (or cysteine side-chain), taken universally as 0.38 nm; α is the cosine of bond-angle supplements for the freely rotating chain model, which was set to a value of 0.8, $2L^2$ term accounts for the size of nitroxide spin-labels, which are considered flexible with the root mean square deviation from the point of attachment of L = 0.35 nm.

III. Approximating distances distributions by the sum of two Gaussians:

All distance distributions were generated from the baseline-corrected experimental data by the L-curve Tikhonov regularization and then refined by minimization of maximum entropy functional (MEM) that included linear baseline correction term. The distributions were clearly bimodal they were approximated by sums of two Gaussians as:

$$P(r) = \frac{x}{\sqrt{2\pi}W_1} \exp\left[-\frac{(r-R_1)^2}{2W_1^2} \right] + \frac{1-x}{\sqrt{2\pi}W_2} \exp\left[-\frac{(r-R_2)^2}{2W_2^2} \right] \qquad \text{(S2)}$$

Here, $P(r)$ is the approximation to distance distributions; W_k (k=1,2) is the "standard deviation" for each Gaussian, which is a well-defined measure of its

width; the R_k are the maxima of Gaussians; the parameter x gives the fraction of the first Gaussian distribution and $1\text{-}x$ that of the second. Equation S2 is normalized so the integral of $P(r)$ with respect to r is unity. The fitting was carefully performed by trial and error to optimize the fit. The R_k were allowed to deviate only slightly from the visible positions of the two peaks; then W_k and x were varied to approximate the distribution. Since the reconstructed $P(r)$'s generally deviate somewhat from the actual distributions, the fitting was considered as adequate after approximating the shapes of the major part of the original $P(r)$'s (except at the very edges, which are the most prone to reconstruction artifacts) with no more than 10% error.

(The tables in the main text use FWHM's for all ΔR's; i.e. for Gaussians $\Delta R_k = 2(2\ln 2)^{1/2} W_k \cong 2.355 W_k$, k = 1,2).

IV. Protein deuteration as the mean to access very long distances

Protein deuteration was used to help measure distances greater than 50 Å. This was an improvement for 24/61 and 24/72 mutants compared to (Ref. S5) and was essential for 24/83 mutant. We illustrate this by showing just two examples (Fig. S3) obtained for 24/72 in SDS and 24/83 in lipidic bicelles. Note that SDS and the buffer were also deuterated, as well as the bicelles and liposomes. The protein deuteration was estimated as 70%, deuterated compounds have been at least 98% enriched. Some lipids (DHPC) however were not deuterated.

This is the first example demonstrating the advantages of deuterating proteins to increase the signal-to-noise ratio or the range of distances measurable by pulse dipolar ESR. Protein deuteration greatly advances the range of distances which is especially important for membrane proteins, for which the distance range is typically limited by approximately 40-50 Å, however see Ref. S5 wherein deuterated lipids were used.

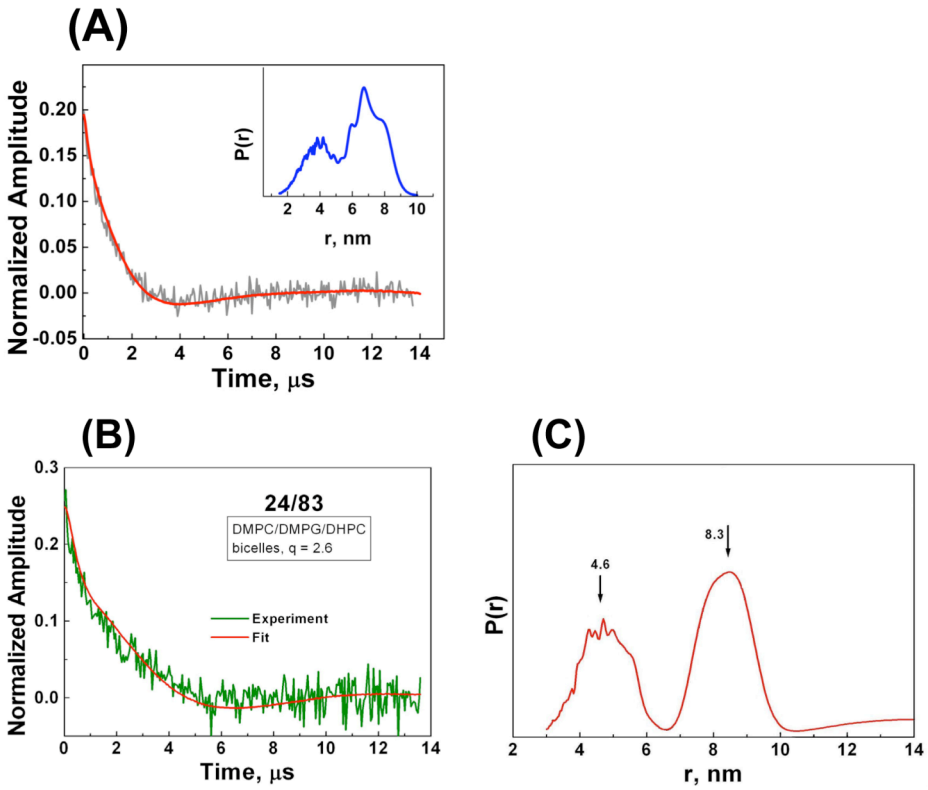

Figure S3. (A) The experimental time-domain data for 70% deuterated A30P αS mutant spin-labeled at positions 24 and 72 and reconstituted in SDS-d25 using deuterated NMR buffer. (B) The experimental time-domain data (green) for deuterated WT αS spin-labeled at positions 24/83 and reconstituted into bicelles. The fit (red) is based on distance distribution (C) produced by MEM. Protein deuteration allowed recording dipolar signal on a time scale as long as 14 μs.

S1. Chiang, YW, Borbat, PP Freed, JH (2005) The determination of pair distance distributions by pulsed ESR using Tikhonov regularization. *J Magn Reson* **172**: 279-95.

S2. Chiang, YW, Borbat, PP Freed, JH (2005) Maximum entropy: a complement to Tikhonov regularization for determination of pair distance distributions by pulsed ESR. *J Magn Reson* **177**: 184-96.

S3. Milov, AD, Maryasov, AG, Tsvetkov, YD, Raap, J (1999) Pulsed ELDOR in spin-labeled polypeptides. *Chem Phys Lett* **303**: 135-143.

S4. Sung, YH Eliezer, D (2007) Residual Structure, Backbone Dynamics, and Interactions within the Synuclein Family. *J Mol Biol* **372**: 689-707.

S5. Georgieva E. R., Ramlall T.F., Borbat P.P., Freed J.H., Eliezer D. Membrane-bound alpha synuclein forms an extended helix: Long-distance pulsed ESR measurements using vesicles, bicelles, and rodlike micelles, JACS, 130, 12856-12857, 2008